Pergamon

Bioorganic & Medicinal Chemistry 9 (2001) 2461–2466

BIOORGANIC & MEDICINAL CHEMISTRY

Specific Host–Guest Interactions in a Protein-Based Artificial Transaminase

Dietmar Häring and Mark D. Distefano*

Department of Chemistry, University of Minnesota, Minneapolis, MN 55455, USA

Received 2 April 2001; accepted 5 June 2001

Dedicated to Professor Peter B. Dervan in recognition of his pioneering work in the fields of bioorganic chemistry and molecular recognition and for his distinctive qualities as a scientific mentor

Abstract—Artificial enzymes can be created by covalent attachment of a catalytic active group to a protein scaffold. Recently, we assembled an artificial transaminase by conjugation of intestinal fatty acid binding protein (IFABP) with a pyridoxamine derivative via a disulfide bond; the resulting construct catalyzed a transamination reaction 200-fold faster than free pyridoxamine. To identify the origin of this increased catalytic efficiency computer modeling was first used to identify two putative residues, Y14 and R126, that were in close proximity to the γ-carboxylate group of the substrate, α-ketoglutartate. These positions were mutated to phenylalanine and methionine, respectively, and used to prepare semisynthetic transaminases by conjugation to pyridoxamine (Px) or an *N*-methylated derivative (MPx). Kinetic analysis of the resulting constructs showed that the R126M mutation reduced substrate affinity 3- to 6-fold while the additional Y14F mutation had a negligible effect. These results are consistent with a model for substrate recognition that involves an electrostatic interaction between the cationic guanidinium group of R126 and the anionic carboxylate from the substrate. Interestingly, one of the conjugates that contains an *N*-methylated pyridoxamine catalyzes a transamination reaction with a k_{cat}' value of 1.1 h^{-1} which is the fastest value for k_{cat} we have thus far obtained and is 34-fold greater than that for the free cofactor in the absence of the protein.

Introduction

The search for rational designed biocatalysts with desired catalytic activities and tailored substrate selectivities has stimulated the development of exciting systems such as catalytic antibodies,[1] coenzyme-amino acid chimeras[2] or semisynthetic enzymes.[3] Protein-based systems are particularly attractive scaffolds for the assembly of new catalysts because their tertiary structure allows many interactions with substrates. Using established recombinant DNA methodologies these scaffolds can be designed at will. We have focused on a class of proteins known as fatty acid binding proteins (FABPs) that possess a large cavity for ligand binding.[4,5] For example, intestinal fatty acid binding protein (IFABP) forms a cavity of 600 $Å^3$, in which fatty acids can be completely sequestered from solvent. Its well established structure and easy overexpression of mutants make this protein a versatile host for rational design by molecular modeling and genetic engineering.

Recently, we assembled an artificial transaminase by conjugation of IFABP with a pyridoxamine derivative (Px) via a disulfide bond to Cys60 inside the cavity.[6] A MOLSCRIPT[7] representation of this construct is shown in Figure 1. That enzyme mimic, denoted here as IFABP-Px, catalyzed the enantioselective transamination of α-ketoglutarate and various amino acids. A significant increase (ca. 200-fold) in catalytic efficiency (k_{cat}/K_M) was observed with IFABP-Px compared to the free pyridoxamine. Kinetic analysis indicated that the turnover number, k_{cat}, of the protein conjugate was approximately 4-fold greater than that for the free cofactor whereas a 50-fold increase in substrate affinity (K_M) for the protein-based host–guest system was found. Since the cofactor is tethered inside the cavity of IFABP and the substrates are completely surrounded by the protein during catalysis, the modulation of catalytic efficiency we observed mediated by the protein host is not surprising. To improve the efficiency of these systems, we are interested in introducing functional groups via mutagenesis of the protein interior that will participate in both catalysis and substrate recognition. Recently we introduced lysine residues into the IFABP cavity at two positions and demonstrated that this new functionality participated in covalent catalysis, altered the rate versus pH profile and increased catalytic efficiency as much as 4200-fold.[8] However, it is also desirable to identify existing residues from the protein host

*Corresponding author. Tel.: +1-612-624-0544; fax: +1-612-626-7541; e-mail: distefan@chem.umn.edu

0968-0896/01/$ - see front matter
PII: S0968-0896(01)00218-8

that form specific interactions with the reaction substrates. If this could be determined, it would then allow the specificity of these artificial transaminases to be altered in a predictable manner.

As noted above, in the original conjugate IFABP-Px, a significant increase in substrate affinity was observed;[9] here, we examine the origin of this effect. Computer modeling was first used to identify two putative residues, Y14 and R126, that were in close proximity to the γ-carboxylate group of the substrate, α-ketoglutartate. We hypothesized that at least one of these amino acids interacted with the substrate-derived carboxylate via electrostatic or hydrogen bonding interactions. These positions were mutated to phenylalanine and methionine, respectively, and used to prepare semisynthetic transaminases by conjugation to pyridoxamine (Px) or an *N*-methylated derivative (MPx). Kinetic analysis of the resulting constructs showed that the R126M mutation reduced substrate affinity 3- to 6-fold while the additional Y14F mutation had a negligible effect. These results are consistent with a model for substrate recognition that involves an electrostatic interaction between the cationic guanidinium group of R126 and the anionic carboxylate from the substrate.

Results

Molecular modeling

The crystal structure of IFABP[10] was used as a starting point to generate computational models of IFABP-Px. The pyridoxal derivative was linked to Cys60 and its conformation energy-minimized. An α-ketoglutarate molecule was bound to the aldehyde group of Px as a ketimine and again optimized. A model for the overall structure of this complex is shown in Figure 1. Interestingly, the γ-carboxylic acid group was in a position suitable for electrostatic interactions and hydrogen bonding to Arg126 or hydrogen bonding to Tyr14, respectively as shown in Figure 2 (left side).

When these residues were replaced by more hydrophobic isosteric amino acids (R126M and Y14F), the overall orientation of α-ketoglutarate was unchanged (Fig. 2, right side). However, these mutations yielded a more hydrophobic environment and prevented favorable interactions with the γ-carboxylic acid group. The phenyl ring of Phe14 is oriented closer to the α-ketoglutarate in comparison to the 4-hydroxy substituted side chain of Tyr14. This suggests that the hydroxy group prevented such an orientation because of a close contact to the γ-carboxylic acid group.

Recently, we developed a *N*-methylated pyridoxamine conjugation reagent (MPx), which has a permanent positive charge at the pyridine nitrogen.[11] The resulting electron-withdrawing effect should enhance the deprotonation of substrate-pyridoxal aldimine and ketimine intermediates.[12] The above described computational modeling was repeated with this *N*-methylated cofactor. Again, the γ-carboxylic acid group of the ketoglutarate bound to pyridoxal was in a position close the side chain functional groups of Arg126 or Tyr14 as shown in Figure 3 (left side). Interestingly, in this case, the Y14F mutation resulted in a lengthening of the distance between the γ-carboxylic acid group of the substrate and the phenyl ring from F14 (Fig. 3, right side).

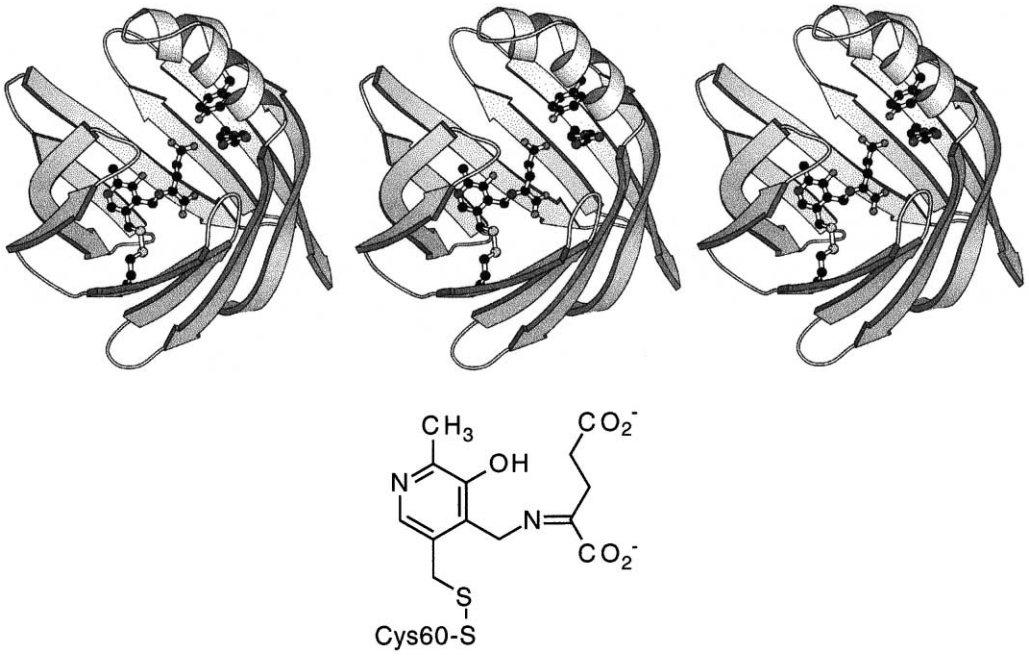

Figure 1. Stereoview of a computational model of a pyridoxamine moiety conjugated to Cys60 of intestinal fatty acid binding protein (IFABP). α-Ketoglutarate is bound to the cofactor with its γ-carboxylic group pointing to Tyr14 and Arg126. The entrance to the protein is in the upper left corner. The model is based on the crystal structure of IFABP and was generated using MOLSCRIPT. The left and central images provide a convergent stereoview while the central and right images give a divergent stereoview.

Conjugate preparation and characterization

In order to test the computational models the IFABP-mutants V60C/R126M and V60C/R126M/Y14F were prepared. Site-directed mutations were introduced in the expression vector of pMON-IFABP recombinant plasmid and the proteins overexpressed in *Escherichia coli* JM105. Both IFABP-mutant proteins were found in the supernatant after cell lysis and purified by ammonium sulfate precipitation, ion exchange chromatography and gel filtration chromatography.[6a,13] Starting from 6 L cultures, 35 mg (V60C/R126M) or 52 mg (V60C/R126M/Y14F), respectively, of homogeneous proteins were isolated. The cofactor was tethered to Cys60 by addition of 10-fold excess 5-(2-pyridyltdithio)pyridoxamine (**1a**) in 20 mM HEPES buffer (pH 7.5) at room temperature as shown in Figure 4. The excess of reagent was removed by gel filtration chromatography and the resulting conjugates IFABP-Px126 and IFABP-Px126/14 showed UV bands of both the protein (280 nm) and the pyridoxamine (326 nm); UV spectra of these two conjugates are shown in Figure 5.

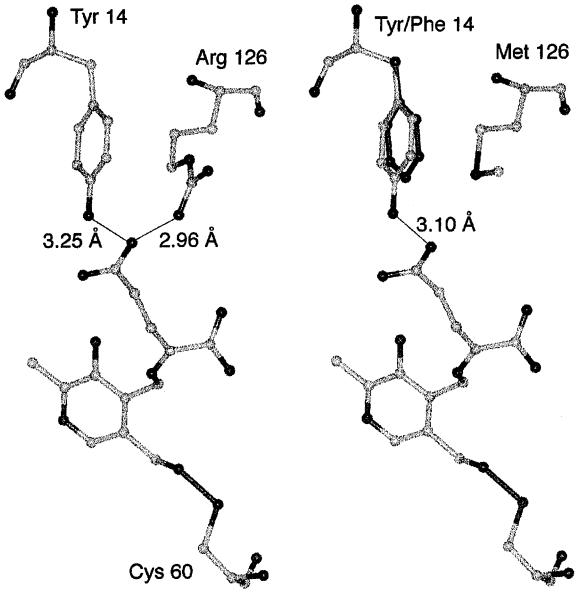

Figure 2. Computer models of the IFABP-Px active site with α-ketoglutarate bound in the ketimine form. The γ-carboxylic group of the substrate interacts with Arg 126 and Tyr 14 (left). The mutants Arg126Met or Arg126Met/Tyr14Phe (black), respectively, are shown on the right side for comparison.

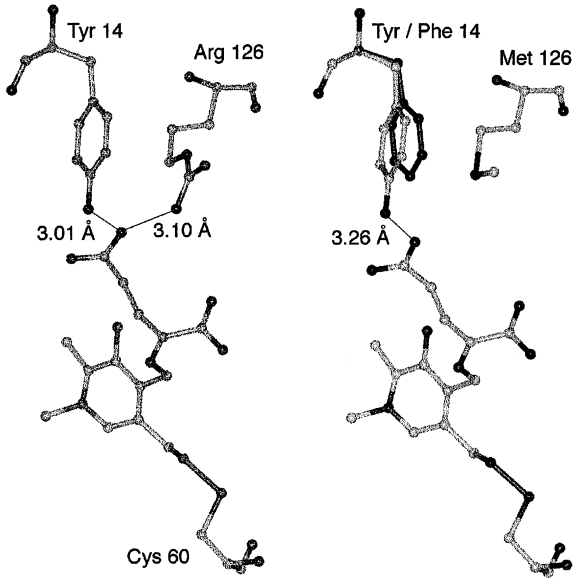

Figure 3. Computer models of the IFABP-MPx active site with α-ketoglutarate bound in the ketimine form. The γ-carboxylic group of the substrate interacts with Arg 126 and Tyr 14 (left). The mutants Arg126Met or Arg126Met/Tyr14Phe (black), respectively, are shown on the right side for comparison.

Using a similar approach as described above, the conjugation reagent 1-methyl-5-(2-pyridyltdithio)pyridoxamine (**1b**, Fig. 4) was used to tether the cofactor via a disulfide bond to Cys60 of IFABP-V60C/R126M and IFABP-V60C/R126M/Y14F. The resulting conjugates, IFABP-MPx126 and IFABP-MPx126/14, were prepared and isolated by gel filtration on a 20 mg scale. UV spectra, shown in Figure 6, of these MPx-containing constructs again displayed bands from both the protein and pyridoxamine but in this case, the pyridoxamine absorbence was red-shifted to a λ_{max} of 338 nm. As previously reported, this shift is characteristic of the *N*-methylated cofactor.

Kinetic analysis of artificial transaminases containing the R126M and Y14F mutations

The newly prepared Px and MPx conjugates catalyzed the transamination of α-ketoglutarate and phenylalanine yielding glutamic acid as shown in Figure 7. All of the conjugates functioned catalytically, performing multiple turnovers in 24 h incubations. Furthermore, the observed catalysis occurred in an enantioselective fashion yielding L-glutamate with an enantiomeric purity of 40–86% *ee*. In general, these enantioselectivities are less than those observed for the parent systems. For example IFABP-Px produces L-glutamate in 95% *ee* while the mutant IFABP-Px126 yields this product in 86% *ee*. The presence of the second mutation in IFABP-Px126/14 further reduces the enantiomeric purity to 67% *ee*; a similar trend was observed with the MPx-based constructs. The kinetic parameters for the transamination reaction catalyzed by the different conjugates were determined by varying the concentration of the keto acid at a constant, saturating, concentration of phenylalanine;[14] these values are tabulated in Table 1 (IFABP-Px conjugates) and Table 2 (IFABP-MPx conjugates). The substrate affinity K_M' of IFABP-Px was lowered by the mutation Arg126Met by a factor of three. The double mutation Arg126Met/Tyr14Phe resulted in an only slightly lower affinity. The k_{cat}'

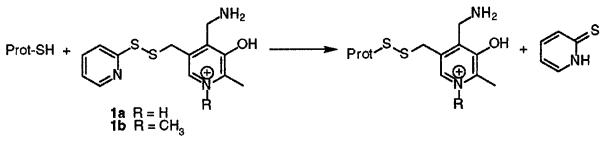

Figure 4. Reaction used for the preparation of IFABP conjugates containing Px or MPx cofactors. Prot-SH is the thiol group from the unique cysteine residue, Cys60, present in IFABP-V60C, used for the preparation of all the constructs described here.

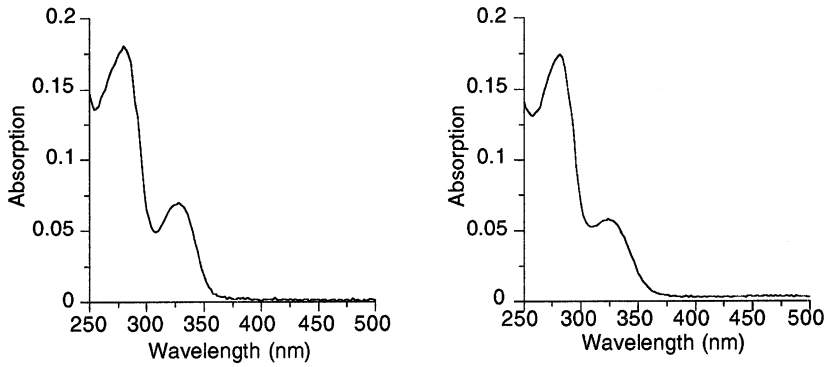

Figure 5. UV spectra of IFABP-Px126 (left) and IFABP-Px126/14 (right).

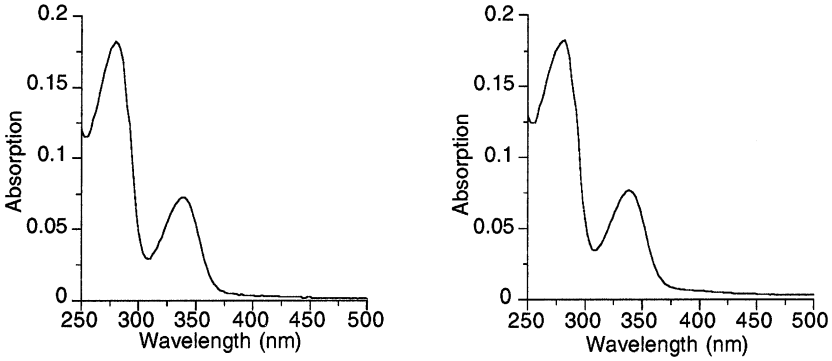

Figure 6. UV spectra of IFABP-MPx126 (left) and IFABP-MPx126/14 (right).

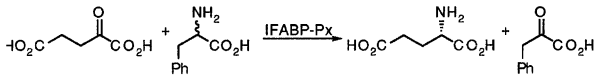

Figure 7. Transamination reaction catalyzed by IFABP-Px conjugates.

values were also influenced by these mutations and found to be down by 40% compared to the original IFABP-Px. The *N*-methylated pyridoxamine conjugates revealed a similar behavior for the substrate affinity. The mutations in position 126 and 14 increased the K_M' values up to seven-fold compared to the original IFABP-MPx. Interestingly, the turnover numbers increased distinctively with IFABP-MPx126 having a nearly 5-fold higher k_{cat}' than IFABP-MPx. This increased turnover is particularly significant since the observed value for k_{cat}' of 1.1 h^{-1} is the fastest value for k_{cat}' we have thus far obtained in any of our semisynthetic enzymes based on IFABP and is 34-fold greater than that for the free cofactor in the absence of the protein.

Table 1. Kinetic parameters for the transamination catalyzed by IFABP-Px mutants

	IFABP-Px	IFABP-Px126	IFABP-Px126/14
K_M' (mM)	1.8±0.5	5.5±1.1	6.0±0.9
k_{cat}' (h^{-1})	0.29±0.02	0.18±0.01	0.11±0.004
k_{cat}'/K_M' ($h^{-1}mM^{-1}$)	0.16	0.03	0.02

Although it is not possible to unambiguously determine the reason for this rate increase without additional experimental data, it is interesting to note that this effect occurs upon removal of the positive charge at position 126 but only with the MPx conjugate. Comparison of the modeling results shown in Figure 2 for the Px conjugates and Figure 3 for the MPx conjugates shows that there are subtle differences in the position and conformation of the pyridoxamine moiety. In the case of the Px conjugates, there is a compression of the distance between the protein (such as position 14) and the substrate-derived γ-carboxylate group while with the MPx conjugates, this distance expands. Such changes may alter the nature of the rate determining step either by affecting the conformation of the substrate–pyridoxamine complex (which must be planar for efficient catalysis) or by perturbing the electrostatics inside the cavity. Additional structural and mechanistic experiments will be necessary to reveal the underlying reasons for these significant rate differences.

Finally, while the data described here clearly supports the idea of a specific interaction between the substrate-derived γ-carboxylate group and Arg126, it is noteworthy that the catalytic efficiency of mutant conjugates lacking Arg126 is still 34- to 68-fold greater that that of the free cofactor. Thus additional interactions between the protein and the pyridoxamine must occur that promote increased catalytic activity. Inspection of the region surrounding the pyridoxamine moiety in the IFABP cavity, modeled in Figure 8, indicates that a

Table 2. Kinetic parameters for the transamination catalyzed by IFABP-MPx mutants

	IFABP-MPx	IFABP-MPx126	IFABP-MPx126/14
K_M' (mM)	6.8±1.3	40±6	48±7
k_{cat}' (h^{-1})	0.23±0.01	1.10±0.06	0.78±0.05
k_{cat}'/K_M' ($h^{-1}mM^{-1}$)	0.03	0.03	0.02

number of residues are in close proximity to the cofactor and substrate. Although IFABP-Px conjugates are still quite primitive catalysts compared to highly evolved natural transaminases, they share important characteristics including an active site architecture that involves multiple interactions between catalyst and substrates that act in concert to increase catalytic efficiency.

Conclusions

Molecular modeling experiments with IFABP-Px identified Arg126 and Tyr14 as possible residues for binding the γ-carboxylic acid group of α-ketoglutarate via hydrogen bonds or electrostatic interactions. Mutant conjugates were produced that lacked these residues. Kinetic analysis suggested that Arg126 but not Try14 was important for binding the substrate. These results demonstrate that molecular modeling can be used to accurately predict the existence of specific interactions in these semisynthetic systems. This should be useful for introducing new residues that can alter the substrate specificity or catalytic efficiency of these artificial enzymes. Finally, it is interesting to note that the construct IFABP-MPx126 which has a significantly increased k_{cat}' value is the product of a strategy that involves both chemical and genetic methods; the protein host was manipulated by mutagenesis while the catalytic properties of the pyridoxamine cofactor were enhanced via chemical synthesis (*N*-methylation). This highlights the enormous flexibility of this 'chemogenetic' approach.

Experimental

Materials

Pyridoxamine dihydrochloride was converted into 5-(2-pyridyltdithio)pyridoxamine (**1a**) as described previously by Kuang et al.[5a] Similarly, 1-methyl-5-(2-pyridyltdithio)pyridoxamine (**1b**) was prepared using a procedure previously reported.[11] The mutagenic primers were obtained from the Microchemical Facility of the Institute of Human Genetics (University of Minnesota). The site-directed mutagenesis kit ('Quick-Change') was obtained from Stratagene. The expression vector pMON-IFABP was used previously for the preparation of IFABP-V60C.[15] Protein purification was carried out at 4 °C unless otherwise noted.

Modeling

Molecular modeling experiments were performed using Insight II 97.0/Discover 3.00 (Molecular Simulations). The potential energy was calculated on basis of a consistent valence forcefield and minimized sequentially by steepest descents and conjugate gradients. The IFABP backbone and all side chains except Cys60, Arg126 and Tyr14 were fixed.

Mutagenesis and protein purification

Site-directed mutations were introduced in the expression vector of pMON-IFABP recombinant plasmid with the QuickChange mutagenesis kit. The sequence for the mutagenic oligomers was 5′-GACCGGAATCA-GAACTTCGAAAAGTTCATGGAG-3′ for Y14F and 5′-GAAGGAGTGGAGGCCAAGATGATCTTTAAG-AAGGAATAG-3′ for R126M. The mutant proteins were expressed in *E. coli* JM105. Cultures were grown in LB

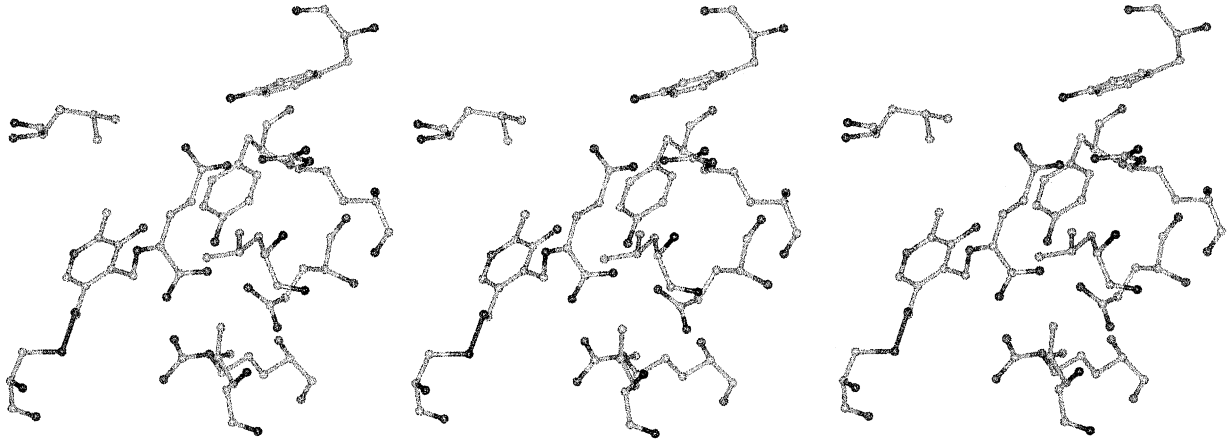

Figure 8. Active site of IFABP-Px in the ketimine form with α-ketoglutarate. The residues Leu72, Tyr14, Tyr117, Arg126, Leu36, Gln115, Arg106 and Leu38 (clockwise, starting form the upper left corner) are shown. Pyridoxamine is bound to Cys60 of IFABP via a disulfide linkage. The left and central images provide a convergent stereoview while the central and right images give a divergent stereoview.

media (6×1 L) with shaking at 37 °C and induced with nalidixic acid for 3–4 h prior to cell harvesting. Upon cell lysis, both mutant proteins were found in the soluble protein fraction. The mutant proteins were purified by ammonium sulfate precipitation followed by ion-exchange chromatography (QAE-Sephadex) and gel filtration chromatography (Sephacryl S-100) as previously described.[6a,13]

Conjugation to pyridoxamine cofactor

Prior to conjugation, the IFABP-mutant proteins were desalted by gel filtration (Biorad P6-DG) and the concentration of free thiol determined by titration with DTNB. The conjugation reagent 5-(2-pyridyldithio)pyridoxamine **1** was added in 10-fold excess and the reaction was allowed to proceed for 18 h at 20 °C in 20 mM HEPES (pH 7.5). The conjugated protein was purified by gel filtration (Biorad P6-DG) and the concentration of pyridoxamine determined by its UV absorbence ($\varepsilon_{326} = 6140\ M^{-1}\,cm^{-1}$ in 6 M guanidine, 20 mM HEPES, pH 7.5). Conjugation with 1-methyl-5-(2-pyridyltdithio)pyridoxamine (**1b**) was performed in an analogous manner. UV spectra of the purified conjugates were recorded at a protein concentration of 10 μM in 20 mM HEPES pH 7.5.

Kinetic analysis

Reactions were performed with 50 μM catalyst, 5 mM phenylalanine (in the case of PMP 5 mM tyrosine was used) and varying concentrations of α-ketoglutarate in 0.2 M HEPES (pH 7.5) at 37 °C. The formation of glutamate was monitored by reversed-phase HPLC.[5a,16]

Acknowledgements

We thank L. J. Banaszak and M. R. Lees for their support with the site-directed mutagenesis and D. P. Cistola for providing pMON-IFABPV60C. The Minnesota Supercomputing Institute provided computer time for the modeling. This work was supported by the National Science Foundation (CHE9807495) and a fellowship of the Deutsche Akademische Austauschdienst (NATO-Programm).

References and Notes

1. (a) Tramontano, A.; Janda, K. D.; Lerner, R. A. *Science* **1986**, *234*, 1566. (b) Pollack, S. J.; Jacobs, J. W.; Schultz, P. G. *Science* **1986**, *234*, 1570.
2. Imperiali, B.; Roy, R. S. *J. Am. Chem. Soc.* **1994**, *116*, 12083.
3. Levine, H. L.; Nakagawa, Y.; Kaiser, E. T. *Biochem. Biophys. Res. Comm.* **1977**, *76*, 64.
4. Banaszak, L.; Winter, N.; Xu, Z.; Bernlohr, D. A.; Cowan, S.; Jones, T. A. *Adv. Protein Chem.* **1994**, *45*, 89.
5. (a) Kuang, H.; Brown, M. L.; Davies, R. R.; Young, E. C.; Distefano, M. D. *J. Am. Chem. Soc.* **1996**, *118*, 10702. (b) Distefano, M. D.; Kuang, H.; Qi, D.; Mazhary, A. *Curt. Opin. Struct. Biol.* **1998**, *8*, 459.
6. (a) Kuang, H.; Davies, R. R.; Distefano, M. D. *Bioorg. Med. Chem. Lett.* **1997**, *7*, 2055. (b) Kuang, H.; Distefano, M. D. *J. Am. Chem. Soc.* **1998**, *120*, 1072. (c) Qi, D.; Kuang, H.; Distefano, M. D. *Bioorg. Med. Chem. Lett.* **1998**, *8*, 875.
7. Kraulis, P. J. *J. Appl. Crystallogr.* **1991**, *24*, 946.
8. Häring, D.; Distefano, M. D. *Bioconjugate Chem.* **2001**, *12*, 385.
9. Transamination reactions catalyzed by free pyridoxamine or protein conjugates thereof follow saturation kinetics and can be fit to a Michaelis–Menton kinetic model with K_M and k_{cat} terms. In the case of free pyridoxamine, K_M is probably equal to the dissociation constant for the ketimine, Schiff base complex. Given that we have been unable to detect substrate binding to FABPs in the absence of the pyridoxamine moiety, we believe that the K_M values obtained with the protein conjugates also reflect the stabilities of the Schiff base complexes. Thus, comparison of these K_M values provides a measure of the increase in substrate affinity due to the presence of the protein component of the construct.
10. Sacchettini, J. C.; Gordon, J. I.; Banaszak, L. J. *J. Mol. Biol.* **1989**, *208*, 327.
11. Kuang, H.; Häring, D; Qi, D.; Mazhary, A.; Distefano, M. D. *Bioorg. Med. Chem. Lett.* **2000**, *10*, 2091.
12. (a) Maley, J. R.; Bruice, T. C. *J. Am. Chem. Soc.* **1968**, *90*, 2843. (b) Maley, J. R.; Bruice, T. C. *Arch. Biochem. Biophys.* **1970**, *136*, 187.
13. Sacchettini, J. C.; Banaszak, L. J.; Gordon, J. I. *Mol. Cell. Biochem.* **1990**, *98*, 81.
14. Although kinetic experiments were performed in the presence of saturating levels of the amino acid substrate, the kinetic parameters obtained cannot be rigorously denoted as k_{cat} and K_M since they were not obtained from extrapolations to infinite amino acid concentration. For this reason, they are designated k_{cat}' and K_M'.
15. Jiang, N.; Frieden, C. *Biochemistry* **1993**, *32*, 11015.
16. Buck, R. H.; Krummen, K. *J. Chromatogr.* **1987**, *387*, 255.